Continuous selective oxidation of methane to methanol over Cu- and Fe- modified ZSM-5 catalysts in a flow reactor

Jun Xu[a,b], Robert D. Armstrong[a], Greg Shaw[a], Nicholas F. Dummer[a], Simon J. Freakley[a], Stuart H. Taylor[a] and Graham J. Hutchings[a*]

[a]Cardiff Catalysis Institute, School of Chemistry, Cardiff University, Main Building, Park Place, Cardiff, CF10 3AT, United Kingdom. Tel: +44 (0) 2920874059, Fax: +44(0) 2090874 030

[b]National Centre for Magnetic Resonance in Wuhan, State Key Laboratory Magnetic Resonance and Atomic and Molecular Physics, Wuhan Institute of Physics and Mathematics, Chinese Academy of Sciences, Wuhan 430071, China

*Corresponding Author – Hutch@cardiff.ac.uk

Abstract

The selective oxidation of methane to methanol is a key challenge in catalysis. Iron and copper modified ZSM-5 catalysts are shown to be effective for this reaction using H_2O_2 as the oxidant under continuous flow operation. Co-impregnation of ZSM-5 with Fe and Cu by chemical vapour impregnation yielded catalysts that showed high selectivity to methanol (> 92% selectivity, 0.5 % conversion), as the only product in the liquid phase. The catalysts investigated did not deactivate during continuous reaction, and methanol selectivity remained high. The effect of reaction pressure, temperature, hydrogen peroxide concentration and catalyst mass were investigated. An increase in any of these led to increased methane conversion, with high methanol selectivity ($\geq$ 73 %) maintained throughout. Catalysts were characterised using DR-FTIR, DR-UV-Vis and ^{27}Al MAS-NMR spectroscopy.

Keywords: Methane; methanol; selective oxidation; ZSM-5; hydrogen peroxide; chemical vapour impregnation

1. Introduction

Natural gas has been hailed as a bridging feedstock for society's transition away from a petroleum-dependent economy [1]. However, the direct catalytic upgrading of its principal components; methane and ethane, to oxygenated products has yet to be realised under mild, environmentally benign conditions. Whilst processes for conversion of methane to higher value products have been commercialised, high substrate stability (ΔH_{C-H} = 439.57 kJ mol^{-1}) means that harsh conditions are often employed for activation [2, 3]. Direct upgrading of methane via oxidation to a more energy dense product, such as methanol, is therefore an attractive prospect. Such a process must operate under mild reaction conditions to prevent further oxidation of methanol to products like formic acid and CO_2. Several approaches to methane oxidation have been reported. The enzymatic direct

oxidation of methane to methanol has been studied, with metalloenzymes shown to perform this reaction selectively under mild conditions with molecular oxygen as the terminal oxidant [4, 5]. This has stimulated the search for synthetic analogues of these enzymes' active sites [6, 7]. Indeed, the gas phase oxidation of methane over Cu- modified zeolites activated in O_2 [8-14] or NO/N_2O [15] has also been studied, with proposed active sites for the O_2 treated catalysts not unlike the binuclear Cu site found in methane monooxygenase enzymes. Meanwhile non- catalytic activation using N_2O/O_2 treated Fe/ZSM-5 has also been reported (with α-oxygen as the *in situ* generated oxidant) [16-18]. Periana and co-workers have extensively studied the oxidation of methane in acidic media –yielding methyl esters at temperatures of < 200 ºC [19-21]. These indirect, methyl ester- yielding processes typically require homogeneous metal complexes which activate methane through electrophilic attack of the C-H bond, affording high reaction selectivity yet incurring additional hydrolysis steps to yield methanol. Such homogeneous processes have been extensively reviewed by Periana *et al* and Shilov *et al* [22, 23] and heterogenised by Schüth and co-workers [24, 25]. A number of homogeneously [26-28] and heterogeneously [29-32] catalysed aqueous processes for the direct oxidation of methane with H_2O_2 have recently been reported. These benefit from the clean decomposition of the oxidant to H_2O as an environmentally benign byproduct. The importance of efficient, selective utilisation of methane as a feedstock for the synthesis of bulk chemicals is explored in recent reviews of the catalytic upgrading of methane [33-37]. Unfortunately despite extensive research in the field, no approach has yet been deemed commercially viable, with methanol still produced through an energy intensive two-step process which proceeds via synthesis gas.

It has previously been reported that ZSM-5 materials containing trace amounts of iron (as dimeric μ-oxo- hydroxo iron species) can catalyse the direct conversion of methane and ethane to oxygenated products, utilizing hydrogen peroxide as the oxidant [31, 32, 40-42]. The oxidation of methane to methanol was shown to proceed via formation of methylhydroperoxide (CH_3OOH), and deep oxidation to formic acid and CO_2 was observed [31]. Appreciable methane conversion (10%) and high oxygenate selectivity (> 90%) have been reported at temperatures as low as of 50 ºC. Furthermore, incorporation of Cu^{2+} into the reaction as either a homogeneous additive or heterogeneous component

of the zeolite catalyst allows tuning of reaction selectivity to favour methanol (> 85%) as the major product. Catalytic reaction pathways determined for the oxidation of methane with H_2O_2 are shown in Scheme 1 [31]. Previous studies have suggested that the intrinsic activity of ZSM-5 is derived from the presence of octahedral (extra framework) Fe species, formed during high temperature activation of the zeolite. The role of Cu^{2+} in effecting high primary product selectivity has been studied, and is attributed to catalytic termination of hydroxyl radicals [43].

In this paper we aim to translate the catalyst system from operation in a batch autoclave to a continuous flow reactor in order to further study catalyst deactivation and determine whether high selectivity to methanol might be achieved under mild reaction conditions.

2. Experimental

2.1 Catalyst preparation

Fe and Cu were impregnated onto ZSM-5 (*Zeolyst*, SiO_2/Al_2O_3 = 23, 30 or 80) via chemical vapour impregnation (CVI) according to the procedure previously reported [41, 44]. NH_4-ZSM-5 was calcined in a flow of air (550 °C, 20 °C min^{-1}, 3 h) to yield H-ZSM-5. This was then either (i) activated in static air (3 h, 550 °C) and tested without further modification or (ii) modified through chemical vapour impregnation. The procedure for simultaneous impregnation of ZSM-5 with 1.5 wt% Fe and 1.5 wt% Cu follows;

H-ZSM-5 (3.5 g) was dried at 150 °C for 2 h under continuous vacuum. Once dried, H-ZSM-5 (1.95 g) was added to a Schlenk flask followed by $Cu(acac)_2$ (Sigma Aldrich, 99.9% purity, 0.103 g, 0.393 mmol) and $Fe(acac)_3$ (Sigma Aldrich, 99.9%, 0.158 g, 0.448 mmol). Following physical mixing of the metal precursors and zeolite, the dry mixture was heated to 150 °C under continuous vacuum (*ca.* 10^{-3} mbar) for 2 h (1 h at 140 °C for monometallic Cu catalysts). The sample was then allowed to cool to ambient temperature and calcined in static air (550 °C, 20 °C min^{-1}, 3h).

Prior to testing, the catalyst was pressed into wafers at a pressure of 20 t/in^2. Wafers were then sieved to form pellets of uniform dimension (20/40 mesh, 800 – 400 μm).

2.2 Catalyst Characterisation

Diffuse reflectance infrared Fourier transform spectroscopy (DRIFTS) was performed using a Bruker Tensor 27 spectrometer fitted with a liquid N$_2$ - cooled MCT detector. Samples were housed in a Praying Mantis high temperature diffuse reflection environmental reaction chamber (HVC-DRP-4) fitted with calcium fluoride windows. Samples were pre-treated prior to spectra acquisition by heating at 200 ºC (10 ºC min^{-1}) in a flow of N$_2$ (10 ml min^{-1}) for 1 h. Scans were collected over the range 4000 cm^{-1} to 1500 cm^{-1}, 4 cm^{-1} resolution, 64 scans against a KBr background.

^{27}Al solid- state NMR experiments were carried out at 7.05 T on a Varian Infinityplus 300 spectrometer. The resonance frequencies were 299.78 MHz and 78.11 MHz for ^{1}H and ^{27}Al respectively. A 4 mm double – resonance probe was employed to acquire ^{27}NMR spectra. The ^{27}Al MAS spectra were acquired using a one- pulse sequence with a short radio frequency (rf) pulse of 0.25 μs (corresponding to a π/ 18 flip angle) and a pulse delay of 0.8 s. The magic angle spinning rate was set to 10 kHz. The chemical shift was referenced to a solution of 1M Al(NO$_3$)$_3$.

UV Vis spectra were collected on a Varian 4000 UV-Vis spectrophotometer. Scans were collected over a wavelength range 200-850 nm, at a scan rate of 150 nm min^{-1}. Background scans were taken using a high purity PTFE disc.

2.3 Catalyst performance evaluation

Catalyst performance was measured in a continuous flow fixed bed stainless steel reactor. A reactor schematic is shown in Figure S1. An aqueous feed containing hydrogen peroxide (*Sigma Aldrich*, typically 0.123 M) was controlled by an HPLC pump (Waters) and methane (*Air Products*, 99.9%)

flow was controlled by a mass flow controller (Brooks). Both were fed down through the catalyst bed (V_{Bed} = 3.6 ml) which was composed of layers of pelleted catalyst and SiC according to the method reported by Al-Dahhan *et al.* [45]. The stainless steel reactor had a total length of 13 cm and internal diameter of 1.6 cm. Liquid and gaseous products were separated in a high pressure liquid gas separator (V_{Total} = 18 ml) and collected periodically for analysis over a 5 hour period. Reactor pressure was maintained using a back pressure regulator.

CO_2 was quantified by GC using a Varian 450-GC instrument fitted with a methaniser-FID and TCD and a CP-Sil 5CB capillary column (50 m x 0.33 mm). Liquid products were quantified by solvent suppressed ^{1}H-NMR on a Bruker Ultrashield 500 MHz spectrometer. A sealed glass capillary containing TMS in $CDCl_3$, calibrated against commercial standards, was added to the NMR tube as an external standard. Hydrogen peroxide was quantified through titration against an acidified solution of $Ce(SO_4)_2$ of known concentration, with Ferroin indicator.

3. Results and Discussion

3.1 Characterisation of Catalysts

It has previously been reported that trace iron in ZSM-5, present as cationic μ-oxo- hydroxo species located at exchange sites, can catalyse the oxidation of methane to methanol by H_2O_2 [31, 43]. Increased catalyst productivity can also be achieved through post- synthesis addition of Fe to ZSM-5 (30) through various techniques [31, 44]. One post- deposition method which has been successfully applied is CVI, a solvent and halide- free vapour deposition technique, which can be applied in the preparation of a range of supported catalysts [41, 44, 46]. Deposition of Fe onto ZSM-5 (30) is reported to lead to formation of a porous FeO_y film on the zeolite surface and within the micropores, whilst Cu deposits as discreet nanoparticles [41]. Both metals are also present as ion exchanged species at Brønsted acid sites [41].

Diffuse reflectance FTIR spectra for a series of Fe-, Cu- and FeCu- ZSM-5 catalysts prepared by CVI are shown in Figure 1. Following deposition of metals, the intensity of the band attributed to OH groups coordinated to Td Al^{3+} in framework positions (3607 cm^{-1}) decreased relative to the bare ZSM-5 [47, 48]. This is consistent with cation exchange at Brønsted sites within the zeolite. In particular, comparison of spectra 1(d) and 1(e) shows increased exchange with increased bimetallic- loading. A small increase in intensity of the band attributed to OH groups coordinated to extra-framework T-atom (3660 cm^{-1}) is also observed, and indicates migration of Fe or Al to extra framework sites when metal impregnated ZSM-5 catalysts are heat treated [49] [50].

^{27}Al MAS NMR spectra for the same ZSM-5 catalysts (Figure 2) are in agreement with DRIFTS characterisation. Addition of Fe and Cu has no effect upon the MFI framework. However, a decrease in intensity of the resonance for Td ^{27}Al in framework sites (55 ppm) was apparent [51]. This suggests the presence of paramagnetic Fe species sited at ion exchange positions [52, 53], which is consistent with the proposed dimeric μ- oxo- hydroxo iron active site. The bridging hydroxyl group (SiOHAl) is the ion exchange position on which the pseudocontact interaction between unpaired electrons from paramagnetic Fe species and framework nuclei (^{27}Al) occurs. This leads to the decrease in the Td ^{27}Al signal. This is also the case when Cu is deposited onto ZSM-5 (30), where a loss in the intensity of the resonance at 55 ppm suggests speciation of copper as exchanged Cu^{2+}. Evolution of extra framework Oh Al sites (0 ppm) in spectra (Figure 2 c-e) is consistent with FTIR spectroscopy studies and suggests a low degree of Al migration from framework (Td) to extra framework (Oh) sites.

Fe speciation on ZSM-5 is known to give rise to four UV-active species. These absorb at; 200-250 nm (isolated Fe^{3+} in framework sites), 250-350 nm (isolated or oligomeric extra framework Fe species in zeolite channels), 350-450 nm (iron oxide clusters) and > 450 nm (large surface oxide species) [54, 55]. Monometallic Fe and bimetallic FeCu catalysts (Figure 3 spectra c-e) show absorbance over the range of wavelengths. Such broad speciation of deposited iron as FeO_y on the zeolite surface and within its micropores is consistent with previous studies on CVI catalysts [41, 44].

A gradual decrease in both surface area and micropore volume was observed for catalysts with increasing metal loading relative to ZSM-5 (30) (Table 1). This was consistent with the decreasing ZSM-5 (30) content per gram of catalyst following deposition of metals.

3.2 Flow reactor studies

For initial studies we tested H-ZSM-5 (30) and modified variants thereof, as these showed high intrinsic activity for methane activation in batch reactor studies [31, 43, 44]. Productivities of 7.4 mol $_{Methane\ converted}$ kg_{cat}^{-1} h^{-1} were previously reported for H-ZSM-5 (30) in a batch reactor under the following test conditions; 27 mg catalyst, 0.5 M H_2O_2 / 5000 µmol, 30 bar CH_4, 50 °C, 0.5 h [31]. When tested under continuous operation the same catalyst shows a productivity of 0.08 mol $_{Methane\ converted}$ kg_{cat}^{-1} h^{-1} (Table 1). Decreased catalyst productivity implies diffusion limitation under the continuous flow regime. Under stirred batch conditions a far lower catalyst mass (27 mg) was used, at comparable oxidant and substrate concentrations. Under flow conditions due to the high catalyst mass (1.5 g) the reaction is operating outside of the kinetic regime. Total oxygenate selectivity (combined CH_3OOH, CH_3OH and $HCOOH$ selectivity) is comparable between reactor regimes (92 % under flow vs 95 % in batch [31]) though secondary oxidation products are favoured under continuous conditions, with CH_3OOH, CH_3OH and $HCOOH$ selectivities of 1.6, 8.7 and 81.6 % respectively. These selectivities are compared with 17.7, 15.4 and 44.0 % reported in batch studies [31]. High formic acid selectivity is consistent with the catalytic nature of the oxidation of methanol to formic acid coupled with the relatively high catalyst: product ratio observed in the fixed bed reactor. An H_2O_2 used/ products ratio of 10: 1 suggests efficient oxidant utilisation under flow conditions, as this compares with 24 : 1 previously reported under batch conditions [41]. The effect of increased substrate and oxidant concentration within the catalyst bed is further explored later in this paper.

Addition of Cu^{2+} shifts the product distribution to favour methanol (89.1% selectivity) with comparable TOF (h^{-1}) (Table 1) to the proton form zeolite. We therefore suggest that the catalysis is consistent with previous studies [31, 40, 43]. Post synthesis deposition of active metal (1.5 wt% Fe) to ZSM-5 (30) leads to increased H_2O_2 decomposition and effects a decrease in reaction rate. This is in

poor agreement with batch studies [31]. With 98% oxidant decomposition it is probable that the reaction is operating under oxidant lean conditions towards the end of the catalyst bed, and this is effectively slowing the rate of reaction. Through co-deposition of Fe and Cu (1:1 wt ratio, 3 wt % total loading) the productivity of H-ZSM-5 (30) (0.08 mol $_{\text{Methane converted}}$ kg$_{\text{cat}}^{-1}$ h^{-1}) can be maintained whilst also affording high methanol selectivity (92.2 %). In this case high H_2O_2 decomposition (92.9 %) is favourable, as it prevents deep oxidation to CO_2 farther through the catalyst bed. Once more the molar ratio of H_2O_2 decomposed: products formed were comparable to previous studies at 26: 1. Surprisingly, no primary product (CH_3OOH) was observed in the product stream of Fe- and FeCu /ZSM-5 catalysed reactions. This is likely to be due to the high Fe: product ratio, as methylhydroperoxide is known to undergo facile catalytic conversion to methanol over Fe/ZSM-5 [43].

Although monometallic Cu/ZSM-5 (30) showed comparable rates of methane conversion, methanol selectivity and higher TOF (h^{-1}) values per mol$_{\text{Fe}}$ (Table 1), previous batch studies have shown bimetallic FeCu/ZSM-5 (30) catalysts to be more productive when this reaction is performed under non- diffusion limited conditions [31]. The bimetallic catalyst 1.5% Fe 1.5% Cu/ZSM-5 (30) was assessed for on-line stability over 10 h of continuous operation (Figure 4). For this, and further studies, a lower bed loading (0.25 g) was used to minimise diffusion limitations. Following a 1 h stabilisation period, a steady state (0.27% conversion, 0.26 mol$_{\text{Methane converted}}$ kg$_{\text{cat}}^{-1}$ h^{-1}, ± 0.022) was attained. Once more, two reaction products were detected; methanol and CO_2 at selectivities of 80 % and 20 % respectively. At this lower catalyst loading 38 % H_2O_2 remained in the reactor liquid exit stream. The decreased oxygenate selectivity when compared with the higher 1.5 g bed loading (80 % vs 92%) is attributed to greater availability of oxidant later in the catalyst bed, which increases the propensity towards deep oxidation. Catalysts were stable to deactivation and poisoning by reaction products over the 10 h testing period.

3.3 Reaction Parameter Studies

An important consideration in the design of a catalytic process is the influence of reaction conditions on reaction rate and product selectivity. Selecting 1.5% Fe 1.5% Cu/ZSM-5 (30), the effect of varying; methane pressure, hydrogen peroxide concentration, temperature and catalyst mass were studied, with the results reported in Table 2.

Previous studies have reported that the rate of methane oxidation with ZSM-5 (30) and H_2O_2 has a 1st order dependency upon both substrate and oxidant concentration [43]. The dependence on substrate concentration became nonlinear at higher pressures of methane (> 5 bar, $[CH_4]$ = 0.0058 M, $[H_2O_2]$ = 0.5 M) with the reaction becoming oxidant limited as Rate $_{H2O2\ Conversion}$ >> Rate $_{Methane\ conversion}$ [43]. The rate of methane oxidation shows a strong dependence on methane pressure/ concentration under flow conditions (Table 2, Entries 1-3). By increasing reactor pressure from 10 to 30 bar, catalyst productivity increased by 76%, from 0.17 to 0.30 mol $_{Methane\ Converted}$ kg_{cat}^{-1} h^{-1}. This pressure range equates to an increase in methane solubility from 0.012 to 0.035 M, as calculated using Henry's Law. In contrast to this, an increase in hydrogen peroxide concentration from 0.06 to 0.25 M (Table 2 Entries 4, 2 and 5) effects a 33% increase in productivity from 0.21 to 0.28 mol $_{Methane\ Converted}$ kg_{cat}^{-1} h^{-1}. This is a strong indication that the reaction is operating under diffusion limited conditions. Two additional approaches were used to further enhance methane conversion; increasing the reactor temperature (Table 2 Entries 6, 2 and 7) and increasing the bed loading (Table 2 Entries 8, 9, 10 and 2). Unsurprisingly the rate of methane oxidation increased upon increasing the reaction temperature from 25 to 75 °C, with productivity increasing from 0.22 to 0.34 mol $_{Methane\ Converted}$ kg_{cat}^{-1} h^{-1}, despite decreasing methane solubility. However, hydrogen peroxide was less efficiently incorporated into products as the reactor temperature increased. This suggests that competing decomposition pathways become more favourable with increasing temperature. Methane conversion was also enhanced through increasing the catalyst loading within the fixed bed. Indeed, conversion increased from 0.26 to 0.5% when the catalyst mass was increased from 0.25 to 1.5 g. Due to the non-linear relationship between mass and conversion, this equates to a decrease in productivity from 0.25 to 0.08 mol $_{Methane}$ $_{Converted}$ kg_{cat}^{-1} h^{-1}. Decreasing productivity is another clear indication that the reaction is substrate/ oxidant limited. Future studies into this catalytic system should therefore address facilitating transport

to the active site through use of more concentrated hydrogen peroxide feeds and increased methane pressures. Interestingly, reaction selectivity was relatively insensitive to the variable test conditions studied. Figure 5 correlates conversion and selectivity data from Table 2. High methanol selectivity (> 73%) was maintained despite an increase of conversion. This suggests that methanol is efficiently removed from the catalyst bed into the liquid gas separator, thereby preventing deep oxidation. This is an important result, and a clear indication that greater methanol yields might be achieved without sacrificing reaction selectivity.

3.4 Effect of varying the zeolite acidity

An additional route to increasing methanol productivity is through increasing the active site density of ZSM-5. Given that the dimeric μ- oxo- hydroxo iron active site is proposed to bridge ion exchange sites [31], this might be achieved through post-synthesis deposition of active metal (Fe). However, as shown in Figure 3 Fe speciation is a largely unselective and limited by the zeolite's exchange capacity. Alternatively, an increased density of active sites might be achieved by varying of the parent zeolite's SiO_2/Al_2O_3 ratio. Varying the Brønsted acidity of H-ZSM-5 has previously been explored [31], with a SiO_2/Al_2O_3 ratio of 30 shown to be optimal. Figure 6 shows a clear benefit of increasing the concentration of AlO_4^- (at constant metal loading). For 1.5% Fe 1.5% Cu/ZSM-5, a decrease in SiO_2/Al_2O_3 enhanced catalyst productivity, whilst also increasing reaction selectivity. Catalyst productivity for FeCu/ZSM-5 (23) was 0.34 mol $_{\text{Methane Converted}}$ kg_{cat}^{-1} h^{-1} which is compared with 0.25 and 0.09 for ZSM-5 (30) and (80) respectively. Added to this, methanol selectivity was highest with the most acidic zeolite (84.7 %), decreasing to 49.5 % when H-ZSM-5 (80) was used as the support. Despite increasing conversion, hydrogen peroxide usage decreased with increasing alumina content (64 % to 57 %). 4.4 % of the oxygen in decomposed H_2O_2 was retained in products when ZSM-5 (23) was used as the support, which falls to 1.1 % for ZSM-5 (80). Acid- stabilisation of H_2O_2 in Fenton's type systems is known [56], and the decrease in H_2O_2 usage is clearly due to such an effect. Meanwhile, the increase in catalyst productivity is attributed to an increase in the population density

of catalytically active Fe sites. A future publication will explore the speciation of active metals on ZSM-5 as a function of exchange capacity and relate this with catalytic performance in the oxidation of short chain alkanes.

4. Conclusions

It has been demonstrated that bimetallic FeCu/ ZSM-5 effectively catalyses the direct oxidation of methane to methanol under continuous flow conditions. Mild reaction conditions and a green oxidant are used without additional promoters or pH control. Reaction selectivity is high towards the primary oxidation products with limited over oxidation (> 73% methanol selectivity), showing low sensitivity to experimental variables. It has been shown that maximising the ion exchange capacity of ZSM-5 benefits reaction rate, selectivity and efficiency. Increasing the efficiency with which the active oxygen is retained in products is a key consideration for future catalyst design studies.

Acknowledgement

8. References

[1] G.A. Olah, Beyond Oil and Gas: The Methanol Economy, Angewandte Chemie International Edition, 44 (2005) 2636-2639.
[2] S.J. Blanksby, G.B. Ellison, Bond dissociation energies of organic molecules, Accounts Chem. Res., 36 (2003) 255-263.
[3] M.A. Pena, J.P. Gomez, J.L.G. Fierro, New catalytic routes for syngas and hydrogen production, Appl. Catal., A, 144 (1996) 7-57.
[4] J. Colby, D.I. Stirling, H. Dalton, SOLUBLE METHANE MONO-OXYGENASE OF METHYLOCOCCUS-CAPSULATUS-(BATH) - ABILITY TO OXYGENATE NORMAL-ALKANES, NORMAL-ALKENES, ETHERS, AND ALICYCLIC, AROMATIC AND HETEROCYCLIC-COMPOUNDS, Biochem. J., 165 (1977) 395-402.
[5] L. Que, W.B. Tolman, Biologically inspired oxidation catalysis, Nature, 455 (2008) 333-340.
[6] A.M. Khenkin, A.E. Shilov, BIOMIMETIC ALKANE OXIDATION IN THE PRESENCE OF IRON COMPLEXES, New Journal of Chemistry, 13 (1989) 659-667.
[7] E.V. Kudrik, P. Afanasiev, L.X. Alvarez, P. Dubourdeaux, M. Clemancey, J.M. Latour, G. Blondin, D. Bouchu, F. Albrieux, S.E. Nefedov, A.B. Sorokin, An N-bridged high-valent diiron-oxo species on a porphyrin platform that can oxidize methane, Nature Chemistry, 4 (2012) 1024-1029.
[8] E.M. Alayon, M. Nachtegaal, M. Ranocchiari, J.A. van Bokhoven, Catalytic conversion of methane to methanol over Cu-mordenite, Chemical Communications, 48 (2012) 404-406.
[9] E.M.C. Alayon, M. Nachtegaal, A. Bodi, M. Ranocchiari, J.A. van Bokhoven, Bis([small mu]-oxo) versus mono([small mu]-oxo)dicopper cores in a zeolite for converting methane to methanol: an in situ XAS and DFT investigation, Physical Chemistry Chemical Physics, 17 (2015) 7681-7693.

[10] P.J. Smeets, R.G. Hadt, J.S. Woertink, P. Vanelderen, R.A. Schoonheydt, B.F. Sels, E.I. Solomon, Oxygen Precursor to the Reactive Intermediate in Methanol Synthesis by Cu-ZSM-5, Journal of the American Chemical Society, 132 (2010) 14736-14738.

[11] N. Beznis, B. Weckhuysen, J. Bitter, Cu-ZSM-5 Zeolites for the Formation of Methanol from Methane and Oxygen: Probing the Active Sites and Spectator Species, Catal Lett, 138 (2010) 14-22.

[12] M.H. Groothaert, P.J. Smeets, B.F. Sels, P.A. Jacobs, R.A. Schoonheydt, Selective Oxidation of Methane by the Bis(μ-oxo)dicopper Core Stabilized on ZSM-5 and Mordenite Zeolites, Journal of the American Chemical Society, 127 (2005) 1394-1395.

[13] S. Grundner, M.A.C. Markovits, G. Li, M. Tromp, E.A. Pidko, E.J.M. Hensen, A. Jentys, M. Sanchez-Sanchez, J.A. Lercher, Single-site trinuclear copper oxygen clusters in mordenite for selective conversion of methane to methanol, Nat Commun, 6 (2015).

[14] P. Vanelderen, R.G. Hadt, P.J. Smeets, E.I. Solomon, R.A. Schoonheydt, B.F. Sels, Cu-ZSM-5: A biomimetic inorganic model for methane oxidation, Journal of Catalysis, 284 (2011) 157-164.

[15] T. Sheppard, C.D. Hamill, A. Goguet, D.W. Rooney, J.M. Thompson, A low temperature, isothermal gas-phase system for conversion of methane to methanol over Cu-ZSM-5, Chemical Communications, 50 (2014) 11053-11055.

[16] K.A. Dubkov, V.I. Sobolev, E.P. Talsi, M.A. Rodkin, N.H. Watkins, A.A. Shteinman, G.I. Panov, Kinetic isotope effects and mechanism of biomimetic oxidation of methane and benzene on FeZSM-5 zeolite, J. Mol. Catal. A-Chem., 123 (1997) 155-161.

[17] M.V. Parfenov, E.V. Starokon, L.V. Pirutko, G.I. Panov, Quasicatalytic and catalytic oxidation of methane to methanol by nitrous oxide over FeZSM-5 zeolite, Journal of Catalysis, 318 (2014) 14-21.

[18] E.V. Starokon, M.V. Parfenov, S.S. Arzumanov, L.V. Pirutko, A.G. Stepanov, G.I. Panov, Oxidation of methane to methanol on the surface of FeZSM-5 zeolite, Journal of Catalysis, 300 (2013) 47-54.

[19] R.A. Periana, D.J. Taube, E.R. Evitt, D.G. Löffler, P.R. Wentrcek, G. Voss, T. Masuda, A Mercury-Catalyzed, High-Yield System for the Oxidation of Methane to Methanol, Science, 259 (1993) 340-343.

[20] R.A. Periana, D.J. Taube, S. Gamble, H. Taube, T. Satoh, H. Fujii, Platinum Catalysts for the High-Yield Oxidation of Methane to a Methanol Derivative, Science, 280 (1998) 560-564.

[21] B.G. Hashiguchi, M.M. Konnick, S.M. Bischof, S.J. Gustafson, D. Devarajan, N. Gunsalus, D.H. Ess, R.A. Periana, Main-Group Compounds Selectively Oxidize Mixtures of Methane, Ethane, and Propane to Alcohol Esters, Science, 343 (2014) 1232-1237.

[22] R.A. Periana, G. Bhalla, W.J. Tenn Iii, K.J.H. Young, X.Y. Liu, O. Mironov, C.J. Jones, V.R. Ziatdinov, Perspectives on some challenges and approaches for developing the next generation of selective, low temperature, oxidation catalysts for alkane hydroxylation based on the CH activation reaction, Journal of Molecular Catalysis A: Chemical, 220 (2004) 7-25.

[23] A.E. Shilov, G.B. Shul'pin, Activation of C–H Bonds by Metal Complexes, Chemical Reviews, 97 (1997) 2879-2932.

[24] R. Palkovits, M. Antonietti, P. Kuhn, A. Thomas, F. Schüth, Solid Catalysts for the Selective Low-Temperature Oxidation of Methane to Methanol, Angewandte Chemie International Edition, 48 (2009) 6909-6912.

[25] M. Soorholtz, R.J. White, T. Zimmermann, M.M. Titirici, M. Antonietti, R. Palkovits, F. Schüth, Direct methane oxidation over Pt-modified nitrogen-doped carbons, Chemical Communications, 49 (2013) 240-242.

[26] A.B. Sorokin, E.V. Kudrik, L.X. Alvarez, P. Afanasiev, J.M.M. Millet, D. Bouchu, Oxidation of methane and ethylene in water at ambient conditions, Catal. Today, 157 (2010) 149-154.

[27] A.B. Sorokin, E.V. Kudrik, D. Bouchu, Bio-inspired oxidation of methane in water catalyzed by N-bridged diiron phthalocyanine complex, Chemical Communications, (2008) 2562-2564.

[28] G.B. Shul'pin, G.V. Nizova, Y.N. Kozlov, L. Gonzalez Cuervo, G. Süss-Fink, Hydrogen Peroxide Oxygenation of Alkanes Including Methane and Ethane Catalyzed by Iron Complexes in Acetonitrile, Advanced Synthesis & Catalysis, 346 (2004) 317-332.

[29] G.B. Shul'pin, T. Sooknoi, V.B. Romakh, G. Süss-Fink, L.S. Shul'pina, Regioselective alkane oxygenation with H2O2 catalyzed by titanosilicalite TS-1, Tetrahedron Letters, 47 (2006) 3071-3075.
[30] M.M. Forde, B.C. Grazia, R. Armstrong, R.L. Jenkins, M.H.A. Rahim, A.F. Carley, N. Dimitratos, J.A. Lopez-Sanchez, S.H. Taylor, N.B. McKeown, G.J. Hutchings, Methane oxidation using silica-supported N-bridged di-iron phthalocyanine catalyst, Journal of Catalysis, 290 (2012) 177-185.
[31] C. Hammond, M.M. Forde, M.H. Ab Rahim, A. Thetford, Q. He, R.L. Jenkins, N. Dimitratos, J.A. Lopez-Sanchez, N.F. Dummer, D.M. Murphy, A.F. Carley, S.H. Taylor, D.J. Willock, E.E. Stangland, J. Kang, H. Hagen, C.J. Kiely, G.J. Hutchings, Direct Catalytic Conversion of Methane to Methanol in an Aqueous Medium by using Copper-Promoted Fe-ZSM-5, Angewandte Chemie International Edition, 51 (2012) 5129-5133.
[32] A.K.M.L. Rahman, M. Kumashiro, T. Ishihara, Direct synthesis of formic acid by partial oxidation of methane on H-ZSM-5 solid acid catalyst, Catalysis Communications, 12 (2011) 1198-1200.
[33] K. Otsuka, Y. Wang, Direct conversion of methane into oxygenates, Applied Catalysis A: General, 222 (2001) 145-161.
[34] C. Hammond, S. Conrad, I. Hermans, Oxidative Methane Upgrading, ChemSusChem, 5 (2012) 1668-1686.
[35] R. Horn, R. Schlögl, Methane Activation by Heterogeneous Catalysis, Catal Lett, 145 (2015) 23-39.
[36] A. Caballero, P.J. Perez, Methane as raw material in synthetic chemistry: the final frontier, Chemical Society Reviews, 42 (2013) 8809-8820.
[37] P. Tang, Q. Zhu, Z. Wu, D. Ma, Methane activation: the past and future, Energy & Environmental Science, 7 (2014) 2580-2591.
[38] N.R. Hunter, H.D. Gesser, L.A. Morton, P.S. Yarlagadda, D.P.C. Fung, Methanol formation at high pressure by the catalyzed oxidation of natural gas and by the sensitized oxidation of methane, Appl. Catal., 57 (1990) 45-54.
[39] A. Hameed, I.M.I. Ismail, M. Aslam, M.A. Gondal, Photocatalytic conversion of methane into methanol: Performance of silver impregnated WO3, Applied Catalysis A: General, 470 (2014) 327-335.
[40] C. Hammond, N. Dimitratos, R.L. Jenkins, J.A. Lopez-Sanchez, S.A. Kondrat, M. Hasbi ab Rahim, M.M. Forde, A. Thetford, S.H. Taylor, H. Hagen, E.E. Stangland, J.H. Kang, J.M. Moulijn, D.J. Willock, G.J. Hutchings, Elucidation and Evolution of the Active Component within Cu/Fe/ZSM-5 for Catalytic Methane Oxidation: From Synthesis to Catalysis, ACS Catalysis, 3 (2013) 689-699.
[41] M.M. Forde, R.D. Armstrong, C. Hammond, Q. He, R.L. Jenkins, S.A. Kondrat, N. Dimitratos, J.A. Lopez-Sanchez, S.H. Taylor, D. Willock, C.J. Kiely, G.J. Hutchings, Partial Oxidation of Ethane to Oxygenates Using Fe- and Cu-Containing ZSM-5, Journal of the American Chemical Society, 135 (2013) 11087-11099.
[42] A.K.M.L. Rahman, R. Indo, H. Hagiwara, T. Ishihara, Direct conversion of ethane to acetic acid over H-ZSM-5 using H2O2 in aqueous phase, Applied Catalysis A: General, 456 (2013) 82-87.
[43] C. Hammond, R.L. Jenkins, N. Dimitratos, J.A. Lopez-Sanchez, M.H. ab Rahim, M.M. Forde, A. Thetford, D.M. Murphy, H. Hagen, E.E. Stangland, J.M. Moulijn, S.H. Taylor, D.J. Willock, G.J. Hutchings, Catalytic and Mechanistic Insights of the Low-Temperature Selective Oxidation of Methane over Cu-Promoted Fe-ZSM-5, Chemistry – A European Journal, 18 (2012) 15735-15745.
[44] M.M. Forde, R.D. Armstrong, R. McVicker, P.P. Wells, N. Dimitratos, Q. He, L. Lu, R.L. Jenkins, C. Hammond, J.A. Lopez-Sanchez, C.J. Kiely, G.J. Hutchings, Light alkane oxidation using catalysts prepared by chemical vapour impregnation: tuning alcohol selectivity through catalyst pre-treatment, Chemical Science, 5 (2014) 3603-3616.
[45] M.H. Al-Dahhan, Y. Wu, M.P. Dudukovic, Reproducible Technique for Packing Laboratory-Scale Trickle-Bed Reactors with a Mixture of Catalyst and Fines, Industrial & Engineering Chemistry Research, 34 (1995) 741-747.

[46] M.M. Forde, L. Kesavan, M.I. bin Saiman, Q. He, N. Dimitratos, J.A. Lopez-Sanchez, R.L. Jenkins, S.H. Taylor, C.J. Kiely, G.J. Hutchings, High Activity Redox Catalysts Synthesized by Chemical Vapor Impregnation, ACS Nano, 8 (2014) 957-969.

[47] F.W. Schuetze, F. Roessner, J. Meusinger, H. Papp, Hydrogen/deuterium exchange on dealuminated H-ZSM-5 zeolites studied by time resolved FTIR spectroscopy, Stud. Surf. Sci. Catal., 112 (1997) 127-134.

[48] A. Zecchina, S. Bordiga, G. Spoto, D. Scarano, G. Petrini, G. Leofanti, M. Padovan, C. Otero Arean, Low-temperature Fourier-transform infrared investigation of the interaction of carbon monoxide with nanosized ZSM 5 and silicalite, J. Chem. Soc., Faraday Trans., 88 (1992) 2959-2969.

[49] L.M. Kustov, V.B. Kazansky, S. Beran, L. Kubelkova, P. Jiru, ADSORPTION OF CARBON-MONOXIDE ON ZSM-5 ZEOLITES - INFRARED SPECTROSCOPIC STUDY AND QUANTUM-CHEMICAL CALCULATIONS, J. Phys. Chem., 91 (1987) 5247-5251.

[50] S. Bordiga, E. Escalona Platero, C. Otero Arean, C. Lamberti, A. Zecchina, Low temperature carbon monoxide adsorption on Na-ZSM-5 zeolites: an FTIR investigation, J. Catal., 137 (1992) 179-185.

[51] C.A. Fyfe, J.M. Thomas, J. Klinowski, G.C. Gobbi, Magic-Angle-Spinning NMR (MAS-NMR) Spectroscopy and the Structure of Zeolites, Angewandte Chemie International Edition in English, 22 (1983) 259-275.

[52] P. Marturano, L. Drozdová, A. Kogelbauer, R. Prins, Fe/ZSM-5 Prepared by Sublimation of FeCl3: The Structure of the Fe Species as Determined by IR, 27Al MAS NMR, and EXAFS Spectroscopy, Journal of Catalysis, 192 (2000) 236-247.

[53] G.A. Webb, The effects of paramagnetism on NMR spectra of nuclei other than protons, Wiley, 1974, pp. 127-142.

[54] M.S. Kumar, J. Perez-Ramirez, M.N. Debbagh, B. Smarsly, U. Bentrup, A. Brueckner, Evidence of the vital role of the pore network on various catalytic conversions of N2O over Fe-silicalite and Fe-SBA-15 with the same iron constitution, Appl. Catal., B, 62 (2006) 244-254.

[55] J. Perez-Ramirez, J.C. Groen, A. Brueckner, M.S. Kumar, U. Bentrup, M.N. Debbagh, L.A. Villaescusa, Evolution of isomorphously substituted iron zeolites during activation: comparison of Fe-β and Fe-ZSM-5, J. Catal., 232 (2005) 318-334.

[56] Y. Jung, J.Y. Park, S.O. Ko, Y.H. Kim, Stabilization of hydrogen peroxide using phthalic acids in the Fenton and Fenton-like oxidation, Chemosphere, 90 (2013) 812-819.
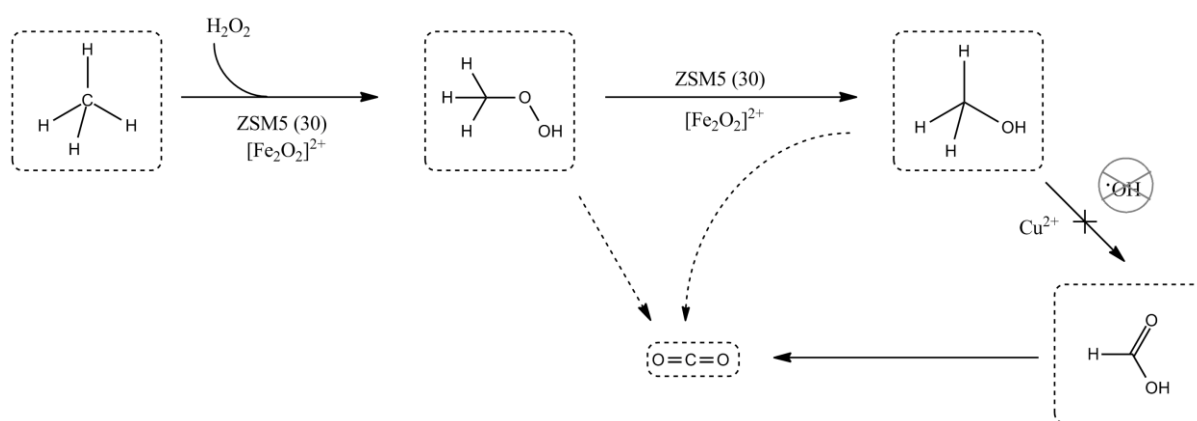
Scheme 1 Reaction scheme for methane oxidation over ZSM-5 (30) catalysts as proposed by previous studies [31, 43].
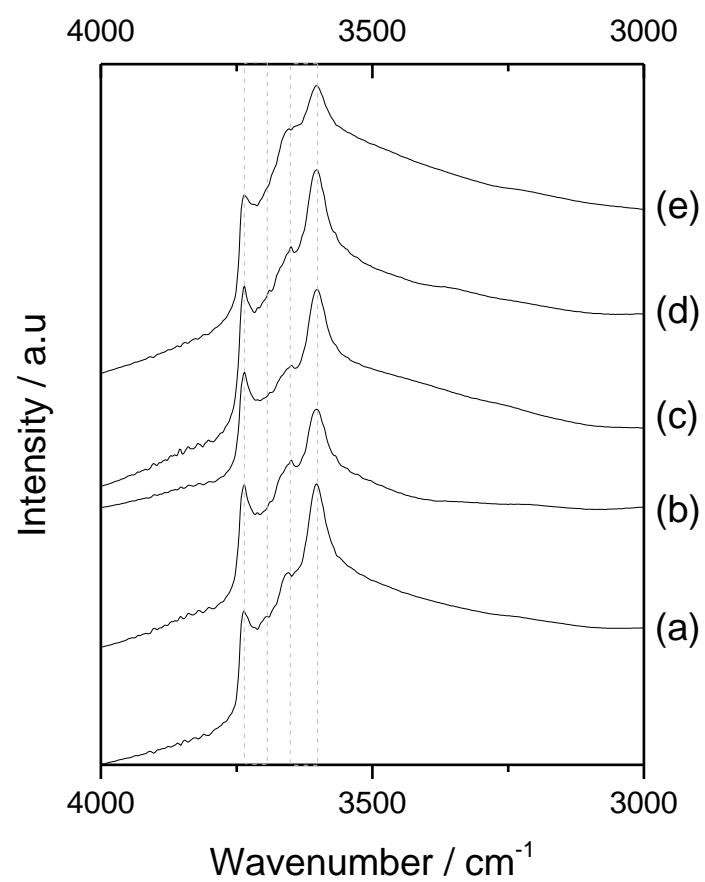
Figure 1 DRIFTS spectra of in the O-H vibration region showing (a) H-ZSM-5 (30), (b) 1.5 % Cu/ZSM-5 (30), (c) 1.5% Fe/ZSM-5 (30), (d) 0.4% Fe 0.4% Cu/ZSM-5 (30) and (e) 1.5% Fe 1.5% Cu/ZSM-5 (30)
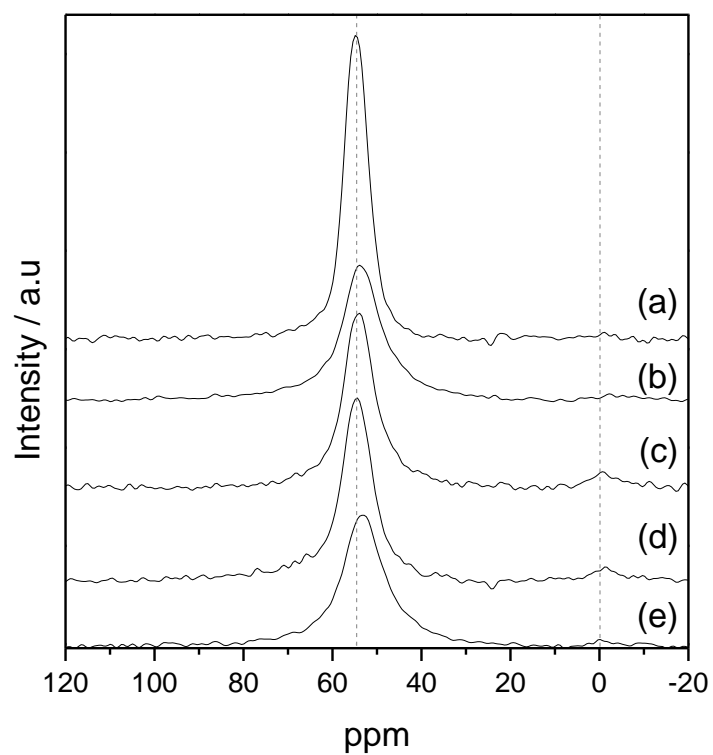
Figure 2 ^{27}Al MAS-NMR spectra showing (a) H-ZSM-5 (30), (b) 1.5 % Cu/ZSM-5 (30), (c) 1.5% Fe/ZSM-5 (30), (d) 0.4% Fe 0.4% Cu/ZSM-5 (30) and (e) 1.5% Fe 1.5% Cu/ZSM-5 (30)

Figure 3 UV-Vis spectra showing (a) H-ZSM-5 (30), (b) 1.5 % Cu/ZSM-5 (30), (c) 1.5% Fe/ZSM-5 (30), (d) 0.4% Fe 0.4% Cu/ZSM-5 (30) and (e) 1.5% Fe 1.5% Cu/ZSM-5 (30)
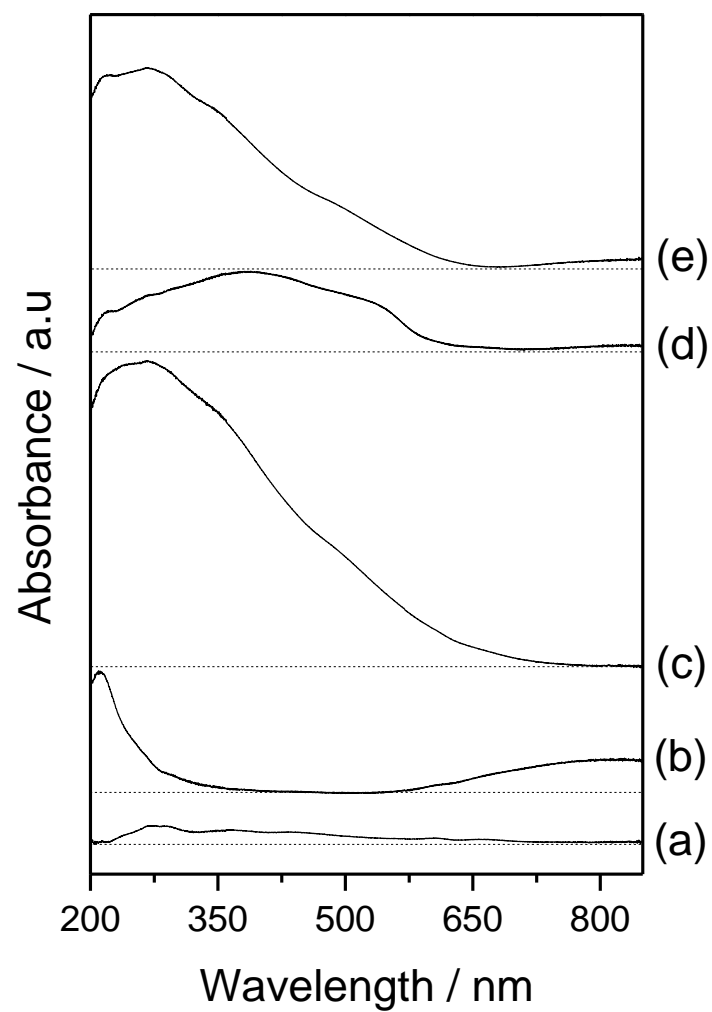
Table 1 Catalytic data for methane oxidation using a range of ZSM-5 (30) catalysts.

Catalyst	Product Selectivity / %				Conversion / %	H_2O_2 used / %	Oxygenate Selectivity / %	Total productivity[b]	H_2O_2 utilisation / %[c]	TOF h^{-1} [d]	S_{BET} / m^2g^{-1}	$V_{micropore}$ $cm^3 g^{-1}$
	CH_3OOH	CH_3OH	HCOOH	CO_2								
H-ZSM-5[a]	1.6	8.7	81.6	8.1	0.5	64.1	91.9	0.081	9.9	26.45	401.0	0.146
1.5% Cu/ZSM-5	1.0	89.1	0.0	9.9	0.4	52.8	90.1	0.065	4.7	21.16	385.2	0.139
1.5% Fe/ZSM-5	0.0	15.1	71.4	13.6	0.2	98.3	86.4	0.032	1.9	0.10	381.7	0.145
0.4% Fe 0.4% Cu/ ZSM-5	0.8	39.2	56.2	3.8	0.3	82.9	96.2	0.049	4.9	0.59	392.7	0.134
1.5% Fe 1.5% Cu/ ZSM-5	0.0	92.2	0	7.8	0.5	92.9	92.2	0.081	3.5	0.30	363.1	0.127

Test conditions; 1.5 g catalyst, $P(CH_4)$ = 20 bar, Flow (CH_4) = 10 ml min^{-1} (0.40 mmol min^{-1}), 0.25 ml min^{-1} of 0.123 M H_2O_2/H_2O, 50 ºC.

[a] H-ZSM-5 (30) 0.014 wt% Fe as determined through ICP-MS

[b] Total productivity measures as $mol_{Product}$ $kg_{catalyst}^{-1}$ h^{-1}

[c] H_2O_2 utilisation measured as % O_2 incorporation from decomposed H_2O_2 into products

[d] TOF (h^{-1}) measured as $mol_{Methane\ Converted}$ mol_{Fe}^{-1} h^{-1}
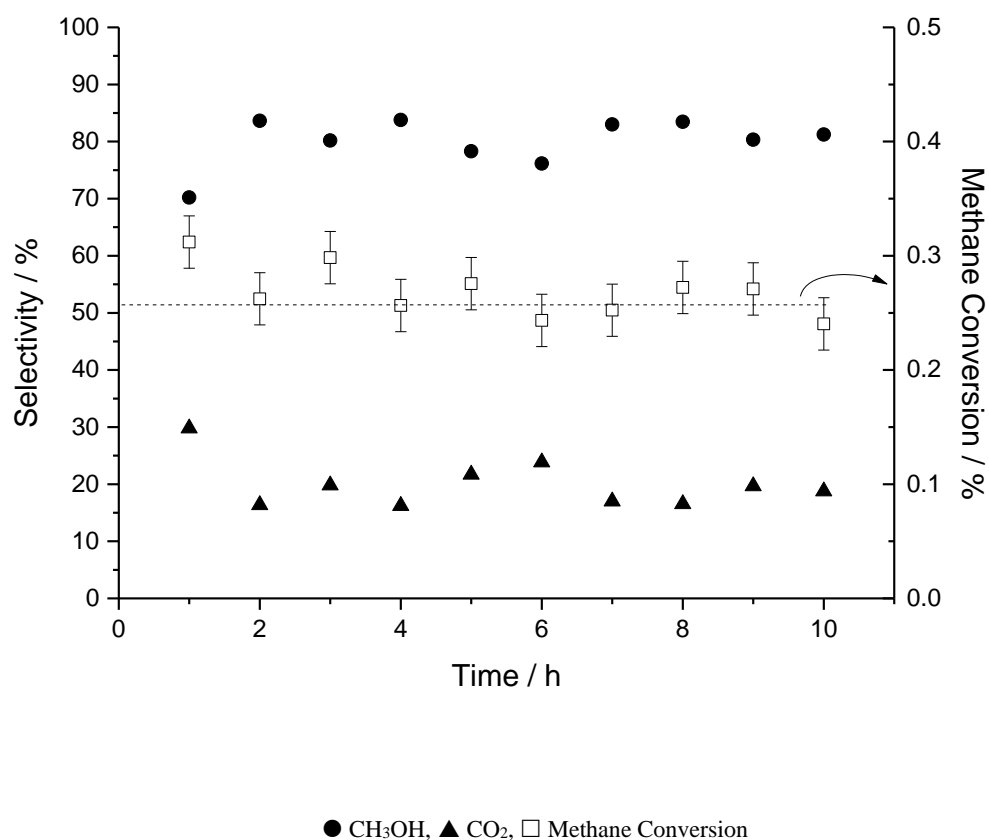
● CH₃OH, ▲ CO₂, □ Methane Conversion

Figure 4. Temporal analysis of methane conversion and reaction selectivity over a 10 h period of assessment.

Test conditions; 0.25 g catalyst, Flow (CH_4) = 10 ml min^{-1}, 0.25 ml min^{-1} of 0.123 M H_2O_2/H_2O, 50 °C.

Table 2 Catalytic data for methane oxidation using 1.5% Fe 1.5% Cu/ZSM-5 (30). The effect of reaction parameters.

Entry	Variable		Calculated $[CH_4]$ / M	Product Selectivity / %				Conversion / %	H_2O_2 used / %	Total productivity[b]	H_2O_2 utilisation / %[c]	TOF h^{-1} [d]
				CH_3OOH	CH_3OH	HCOOH	CO_2					
1	P(CH_4) /	10	0.012	0	74.6	0	25.4	0.18	47.4	0.17	2.8	0.65
2*	bar	20	0.023	0	77.3	0	22.7	0.26	62.1	0.25	3.0	0.94
3		30	0.035	0	73.0	0	27.0	0.31	57.3	0.30	3.1	1.11
4	[H_2O_2] /	0.0615	0.023	0	78.6	0	21.2	0.22	57.6	0.21	5.5	0.80
5	M	0.246	0.023	0	89.4	0	10.6	0.29	67.6	0.28	1.5	1.04
6	Temp /	25	0.038	0	83.5	0	16.5	0.23	26.5	0.22	6.4	0.83
7	ºC	75	0.015	0	81.8	0	18.2	0.35	64.8	0.34	3.4	1.26
8	Mass	0.5	0.023	0	88.0	0	12.0	0.32	74.5	0.15	2.8	0.58
9	Catalyst	1.0	0.023	0	89.6	0	10.4	0.36	80.1	0.09	2.9	0.32
10	/ g	1.5	0.023	0	92.2	0	7.8	0.5	92.9	0.08	3.5	0.30

Standard test conditions; 0.25 g catalyst, P(CH_4) = 20 bar, Flow (CH_4) = 10 ml min^{-1} (0.40 mmol min^{-1}), 0.25 ml min^{-1} of 0.123 M H_2O_2/H_2O, 50 ºC.

[a] H-ZSM-5 (30) 0.014 wt% Fe as determined through ICP-MS

[b] Total productivity measures as $mol_{Product}$ $kg_{catalyst}^{-1}$ h^{-1}

[c] H_2O_2 utilisation measured as % O_2 incorporation from decomposed H_2O_2 into products

[d] TOF (h^{-1}) measured as $mol_{Methane\ Converted}^{-1}$ Mol_{Fe}^{-1} h^{-1}
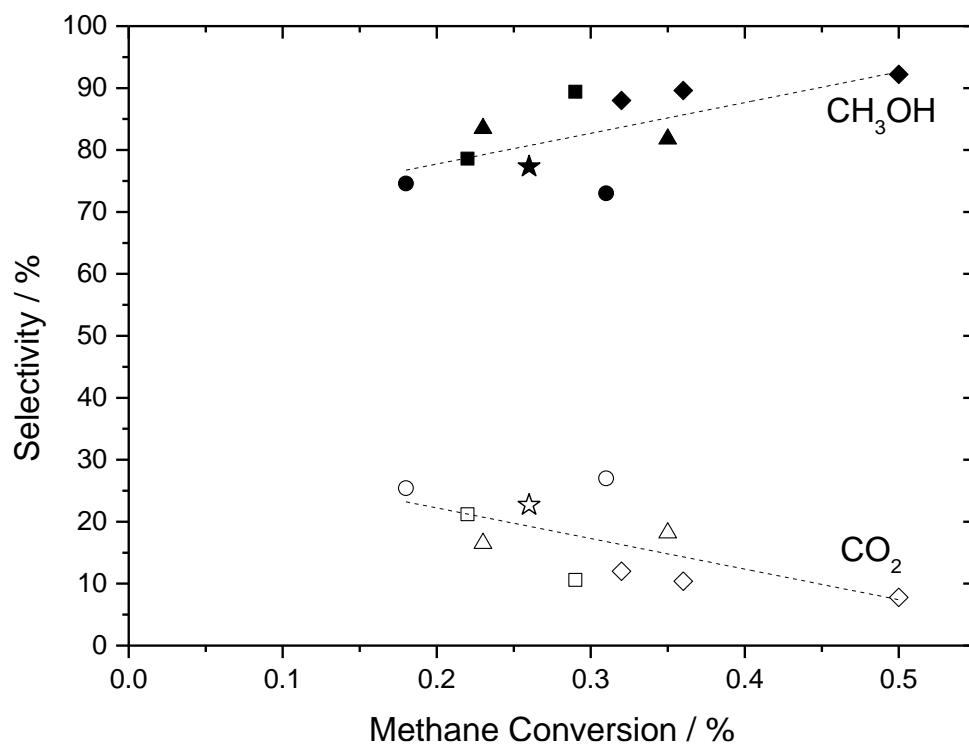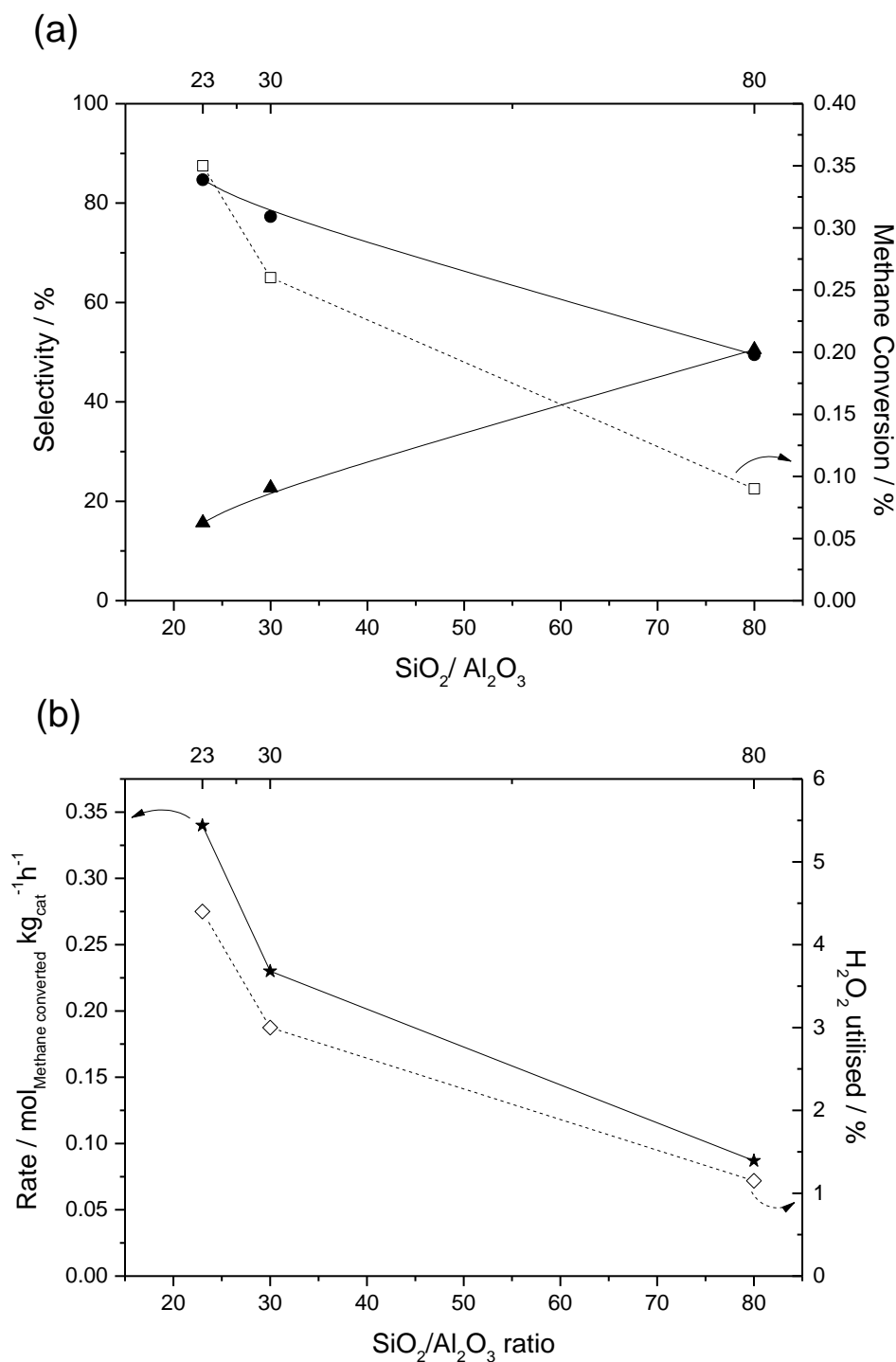
Figure 5 Conversion vs selectivity plots for methane oxidation reactions catalysed by 1.5% Fe 1.5% Cu/ZSM-5 (30)

Symbols represent studies into the effect of; methane pressure (●○), hydrogen peroxide concentration (■□), reactor temperature (▲△), catalyst mass (◆◇) and standard conditions (☆★)

(a) CH_3OH (●), CO_2 (▲) Methane Conversion (□) (b) Rate $_{Methane\ Conversion}$ (★) Efficiency of H_2O_2 utilisation in products (◇)

Figure 6. Methane oxidation over 1.5 % Fe 1.5% Cu/ZSM-5 catalysts where SiO_2/Al_2O_3 = 23, 30 and 80. Showing (a) Reaction selectivity and methane conversion (b) Catalyst productivity and efficiency of H_2O_2 utilisation.

Test conditions; 0.25 g catalyst, $P(CH_4)$ = 20 bar, Flow (CH_4) = 10 ml min^{-1}, 0.25 ml min^{-1} of 0.123 M H_2O_2/H_2O, 50 °C.